International Journal of Multiphase Flow 35 (2009) 398–409

Contents lists available at ScienceDirect

International Journal of Multiphase Flow

journal homepage: www.elsevier.com/locate/ijmulflow

Wave frequency of falling liquid films and the effect on reflux condensation in vertical tubes

U. Gross, Th. Storch *, Ch. Philipp, A. Doeg

Institute of Thermal Engineering, Technische Universität Bergakademie Freiberg, Gustav-Zeuner-Strasse 7, D-09596 Freiberg, Germany

ARTICLE INFO

Article history:
Received 29 July 2008
Received in revised form 11 November 2008
Accepted 3 January 2009
Available online 10 January 2009

ABSTRACT

Visual investigations of effective wave frequency, structure and formation of isothermal and fully developed falling liquid films inside vertical tubes are presented without and with countercurrent flow of vapour. These are supplemented by novel transmissivity measurements leading to considerable improvement of the established wave shape and liquid film structure classifications. In addition, reflux condensation heat transfer data evaluated for the limiting case of zero shear stress are represented in terms of the wave factor. These are correlated with Reynolds and Kapitza numbers and they are interrelated with the observed wave characteristics.

1. Introduction

The first analytical solution of velocity profile and heat transfer across a smooth laminar film has been presented by Nusselt (1916) in his pioneering work with and without the influences of the vapour-side shear stress. Experimental experience confirmed the resulting equation as a lower limit for condensation heat transfer which is found to be enhanced by wave formation and transition to turbulence. The structure of falling liquid films is usually classified to be laminar, laminar-wavy, and turbulent depending on Reynolds, Kapitza and Prandtl numbers.

Two different Reynolds number definitions are common practice, namely $\mathrm{Re} = \dot{M}/(\pi d_i \mu)$, based on film thickness and velocity, and $\mathrm{Re}^* = 4\mathrm{Re}$, derived from tube diameter and superficial velocity of the liquid. The former definition will be applied in this paper and Re^* data from the literature will respectively be transferred to Re. The Kapitza number has been established for classification of the wave activity in falling liquid films honouring Piotr Leonidovich Kapitza, and

$$\mathrm{Re} = 0.6075\mathrm{Ka}^{-1/11} \tag{1}$$

has been compiled as the lower limit for the development of sinusoidal waves (see Kapitza (1948)). Three years earlier, Grimley (1945) published

$$\mathrm{Re} = 0.291\mathrm{Ka}^{-1/8} \tag{2}$$

as the smallest Re number for a wavy liquid film. A literature review regarding the Kapitza number shows some confusion with the various definitions like $\mathrm{Ka} = \mu^4 g/(\rho\sigma^3)$ (Chun and Seban, 1971; Alhussenini et al., 1997; VDI Wärmeatlas, 2006), also common as $\mathrm{Ka}^* = 1/\mathrm{Ka}$, $\mathrm{Ka}^{**} = (1/\mathrm{Ka})^{1/3}$, $\mathrm{Ka}^{***} = S = (1/\mathrm{Ka})^{1/5}$ and $\mathrm{Ka}^{****} = S^* = (3/\mathrm{Ka})^{1/5}$.

The present authors performed extended measurements of local reflux condensation heat transfer coefficients inside a vertical tube. These investigations were focussed on shear stress effects by a countercurrent vapour flow (upwards) on heat transfer across the liquid falling film (downwards). Respective results have been published by Thumm (2000), Thumm et al. (2001), Gross et al. (2002) and Gross and Philipp (2006). These experiments were done very carefully and excellent reproducibility of the results has been obtained, where Nu numbers diverge less than ±1% and ±0.5%, respectively, with water and isopropanol as the working fluids for experiments repeated after two and three years. This allows a well based extrapolation of measured data to zero shear stress. The results are plotted as $\mathrm{Nu}_{\tau\to 0}$ versus Re numbers with the Pr number ranging from 2.6 to 55 as additional parameter. This allows a precise and detailed analysis of condensation heat transfer for smooth laminar and wavy film flow up to developing turbulence.

The present contribution is directed to interrelations between the heat transfer enhancement and typical wave characteristics. In the next sections test rigs, measurement and visualization techniques will be described, starting with a respective literature review. After that the results of visual observations and a classification of wave shapes will be stated.

2. Literature review

2.1. Heat transfer

Correlations of heat transfer measurements in cases of film condensation and/or falling film evaporation have been presented by many scientists, however, mostly for the configurations of vertical wall or the outside of tubes. The ratio between measured heat

* Corresponding author. Tel.: +49 3731 392423.
E-mail address: storch1@iwtt.tu-freiberg.de (Th. Storch).

0301-9322/$ - see front matter © 2009 Elsevier Ltd. All rights reserved.
doi:10.1016/j.ijmultiphaseflow.2009.01.001

transfer coefficients ($Nu_{exp.}$) and those predicted by Nusselt's theory ($Nu_{Nusselt\ 1916}$) is usually expressed by the wave factor (F_{wave}) as:

$$F_{wave} = \frac{Nu_{exp.}}{Nu_{\ Nusselt\ 1916}} \tag{3}$$

Such wave factors have been evaluated from condensation heat transfer data at zero shear stress, as done by Gross and Philipp (2006), see Fig. 1, and they may also be derived from respective correlations. For laminar wavy film condensation, McAdams (1954) and Blangetti (1984) introduced constant wave factors (F_{wave} = 1.28 and 1.15, respectively). Furthermore, wave factors are found to increase with the Re number as reported by Labuntsov (1957), Zozulya (1959) and Uehara (1980) who introduced $F_{wave} \propto Re^{0.04}$, $F_{wave} \propto Re^{0.11}$ and $F_{wave} \propto Re^{0.083}$, respectively. Sofrata (1980), Uehara et al. (1983) and Mitrovic (1990) refined the wave factor calculation by including Ka number effects. In case of laminar wavy film evaporation, Alhusseini et al. (1997) did the same, whereas Chun and Seban (1971) restricted the wave factor calculation on Re number effects similar to Kutateladze's (1963) approach.

2.2. Wave shape and frequency

Formation and structure of falling wavy films have widely been studied in the past and numerous investigations can be found for many liquids and wall surface configurations e.g. by Emmons (1951), Dukler and Bergelin (1952), Brauer (1956, 1971), Zhivaikin and Volgin (1961), Wilke (1962), Ishigai et al. (1972), Portalski (1960, 1963, 1973), Uehara et al. (1983, 1988, 1989), Alekseenko et al. (1994), Al-Sibai (2004) and Koizumi et al. (2005).

Various experimental methods are reported: needle and inductive probes for getting more or less local transients of the wave thickness, some optical methods (shadow graphs, particle image velocimetry (PIV), fluorescence) for cross sectional wave profiles and their development. An overview has recently been given by Clark (2002) who presented the various methods for film thickness measurements, by Lel et al. (2005) concerning local thickness and wave velocity measurements, by Koizumi et al. (2005) regarding dimensionless wave characteristics, and by Drosos et al. (2004) who reported characteristics of developing free falling films. Adomeit (1996), Adomeit and Renz (2000), Adomeit et al. (2000), Al-Sibai et al. (2002a,b), Al-Sibai (2004) and Lel et al. (2005) presented extended studies of the local hydrodynamics of waves and falling films at flat vertical plates (the latter four publications) and inside tubes (the first three ones). In these studies a fluorescence intensity technique has been used for the measurements of film thickness and wave velocity while the velocity distribution inside the film was determined by PIV. Lel et al. (2005) additionally applied the so-called "chromatic confocal imaging method" for measuring the thickness of wavy films. Besides that, Al-Sibai et al. (2002a,b) and Al-Sibai (2004) investigated the instantaneous and local wall to liquid heat transfer (without condensation) by an infrared thermography method. Most recently Schagen et al. (2006) published first measurements of local film thickness and temperature distributions by application of a new method based on luminescence indicators.

Waves on falling liquid films inside tubes are found to exhibit a deterministic or chaotic behaviour depending on Reynolds number, Kapitza number, and entrance length. Occasionally Froude and Weber numbers are also considered in the literature. Various characteristic wave shapes are found by Philipp et al. (2006) who visually investigated water films (at 17.5–21 °C) flowing downward inside a glass tube, as sketched in Fig. 2, with the following conclusions:

- In cases of Re < 7, where liquid water films usually are treated to be smooth, the visual observations show so-called "very small waves", see Fig. 2a, with a closed symmetrical wave crest around the inner tube surface being called "two dimensional". Actually it is difficult to identify a falling liquid film which is entirely smooth without any visible disturbance.
- For 7 < Re < 9 regularly "small waves" are found still being symmetrical, see Fig. 2b.
- For 9 < Re < 13, the wave height is further growing, now forming "large waves" with single bow waves in front of them, see Fig. 2c. Such waves are still two dimensional being, however, not fully circled. The experiments clearly show the development of such waves starting from the top with several "small waves" which step-by-step accumulate and finally disappear forming those large waves.
- For Re > 13 symmetry gets lost, wave crests become inclined and interrupted. Such waves are called to be "two dimensional inclined", i.e. they are two dimensional relative to an inclined coordinate system running down in shape of a horseshoe with an increasing number of bow waves, see Fig. 2d.
- For Re > 15 first "fast waves" are identified which are characterized by accumulation of a large mass of liquid sliding downward very fast. Such waves influence the flow pattern by overtaking and carrying other waves, see Fig. 2e.
- Between Re = 40 and 50 transition from two to three-dimensional wave shape is reported with more or less strong but regular wave height variations which has been illustrated as "basketwork" profile.

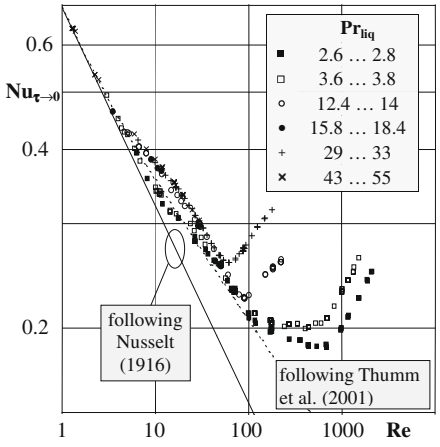

Fig. 1. Condensation heat transfer for the limiting case of zero shear stress.

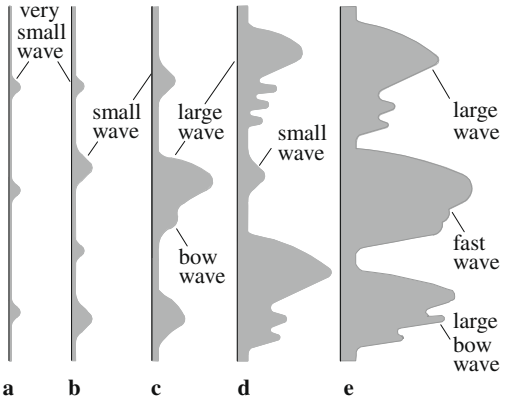

Fig. 2. Classification of wave shapes.

– For even larger Re numbers streak-like and surge-like waves occur with transition to a nearly semi-circled wave front. Wave peaks are now running down helically as visible in slow motion videos. Such streak-like down running waves have also been observed earlier by Adomeit (1996) and Adomeit and Renz (2000) and they clearly found first signs of turbulence from local PIV measurements for dimethylsulfoxide at Re numbers 72 and 85.

Obviously there is more than one possible definition of the wave frequency. Brauer (1956) and Ishigai et al., e.g. considered large waves only (maximum in film thickness, see Fig. 2c–e series) other investigations include occasional small waves and bow waves in addition. Both concepts can be found in the related literature depending on the various measuring methods and research aspects. For getting a systematic overview, around 100 recent publications have been analyzed. The results are found to be wide spread due to the variety of different measuring methods at different distances from the liquid inlet, see Table 1. No systematic dependency of the wave frequency on Re number and no correlation to heat transfer could be found. Wave frequencies are mostly evaluated at locally fixed points. Philipp et al. (2006) did this as well, and the results have been found to be in good agreement with comparable literature data.

One more example: Karapantsios et al. (1989) determined wave frequencies from local film thickness measurements with water (Re = 127–3272). They evaluated spectral density maxima which brought frequencies from 5 to 8 s^{-1}. Using their published film thickness versus time plots we counted the number of wave peaks per second (large and small ones) for comparison. The counted frequency (28 s^{-1}, see Table 1) has been found to be much higher than those published by the authors. The same applies to Koizumi et al. (2000) and Al-Sibai (2004) who investigated the wave frequencies of R-113 (Re = 15–150) and silicone fluids (Re = 2–690).

However, the question is posed which amount of film thickness change is necessary to deliver a significant influence on heat transfer. So far, for a constant liquid mass flow rate at laminar-wavy flow conditions it is obvious that heat transfer coefficients increase along with the number of wave peaks per unit of area and time (frequency) because each wave peak assimilates liquid from a much larger surrounding area. Frequency determination of the large waves is self-evident. But the influence of the frequency of the small waves (between the large ones) on heat transfer is significant due to the fact that the film-thickness change causes the largest effect at locations of smallest film thickness. This was motivation for Philipp et al. (2006) to evaluate wave frequency as the summary of both, large and small waves (without bow waves) and they called it effective wave frequency.

Nevertheless, many interesting results came from all these publications which are, however, not directly applicable to analysis and explanations of the details of measured condensation heat transfer data inside a vertical tube. This is especially true in cases where the visual experiments have been done at plane and also at convex surfaces (outside surface of a tube) or if their quality and/or quantity is not sufficient.

3. Experiments

3.1. Experimental set-up

The experimental set-up consists of a vertical brass tube with the total length and inner diameter of 4.2 m and 28.2 mm, respectively, see Figs. 3 and 4. There are two separately assessable cycles, a liquid and a vapour cycle. In the first one liquid isopropanol penetrates a porous steel section (sintered metal) at the top of the tube and a uniform film is created flowing downward at the inner wall surface. A film separation device is located at the bottom of the tube, and the liquid is re-cycled at constant temperature by a pump to the porous steel section. In the second cycle, vapour is generated in an evaporator or alternatively by heating the film separation device and it is forced to flow upwards countercurrent to the liquid film. For evaluation, particular mass flow rates were measured after liquification by means of Coriolis flow meters with an accuracy of about ±0.15% on the measured value, see Fig. 3.

Local filmwise condensation heat transfer coefficients are measured at the lower end of a water cooled section (total length 1.7 m; entrance length 1.58, see Fig. 3). The remaining part of the tube below the cooling section served as an adiabatic entrance length for the countercurrent vapour flow. The measured heat transfer data have been extrapolated to zero shear stress, see

Table 1
Overview of some measurements at vertical walls and wave frequencies, see Philipp et al. (2006).

	Liquid		Tube (D_i, D_o), flat plate (W)		Film thickness		
	Name	Temperature (°C)	D_i, D_o, W (width) (mm)	Distance from liquid inlet × (m)	Measurement	Re	f (1/s)
Adomeit (1996), Adomeit and Renz (2000), Adomeit et al. (2000)	Dimethyl sulfoxide	37	D_i = 54; 46	1.4	Fluorescence intensity technique		
Ambrosini et al. (2002)	Water	20–30	W = 600	1.7	Electric capacitance		
Karapantsios and Karabelas, 1995	Water	20	D_i = 50	1.77	Parallel-wire conductance		
Karapantsios et al. (1989)	Water	20	D_i = 50	2.5	Parallel-wire conductance	127	28
Koizumi et al. (2000), Koizumi et al. (2001)	R-113	16–19	D_o = 25	0.2–1.2	Video camera and electric capacitance		
	Water	23		0.4 and 1			
Koizumi et al. (2005)	Water silicone		D_i = 30	2.8	Laser fluorescence		
Leuthner (1999)	Water	22–34	D_o = 25.5	1.4	High-frequency impedance needle	75	19
						93	23
						111	29
						128	33
Park and Nosoko (2003)	Water	15–24	W = 205	0.14–0.48	Shadow image		
Park et al. (2004)	Water	15–24	D_i = 9.6	1	Shadow image		
Takahama and Kato (1980)	Water	17	D_o = 44.92	0.3	Needle contact electric capacity	576	40
				0.5–1.7		576	31.7
Takamasa and Hazuku (2000)	Water	15	W = 210	0.234	Laser focus displacement meters	79	20
				>0.133		112	30
Takamasa and Kobayashi (2000)	Water	25	D_i = 26	0.22	Laser focus displacement meter	80	25
				0.4–1.52		80	20
Yu et al. (1995)	Water	22	D_i = 50.8	2	Parallel-wire conductance	75	19

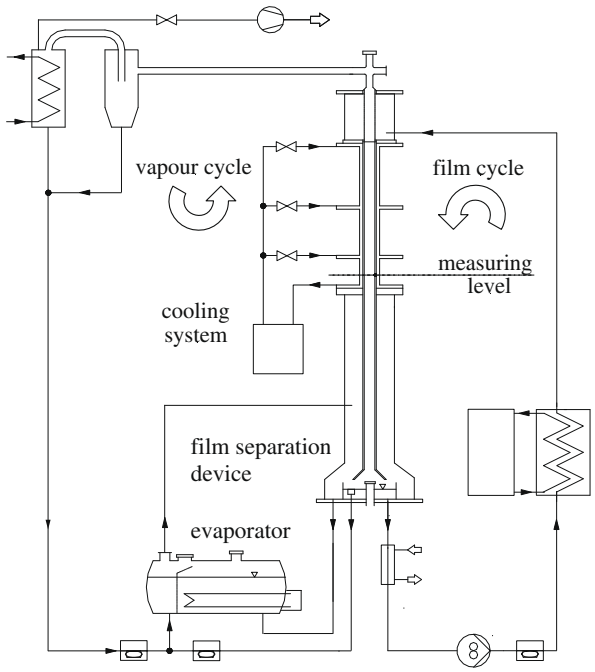

Fig. 3. Schematic drawing of the test facility.

Fig. 1. For more details of the heat transfer experiments see Thumm et al. (2001), Gross et al. (2002) and Gross and Philipp (2006).

For our following visual experiments we used the same test plant, however, under isothermal conditions. Three different arrangements of camera equipment and illumination have been used, see Fig. 4:

- Fig. 4a shows the first set-up with a pencil-like cylindrical camera (PCC, outside diameter 14 mm, 50 half-frames per second) which is centered inside the tube close to the measuring level of the previous condensation heat transfer experiments. Light is supplied through a sight glass at the lower end of the tube. This arrangement has been used for visual observations of an isopropanol film (t = 30.3 °C) without shear stress, i.e. stagnant vapour.

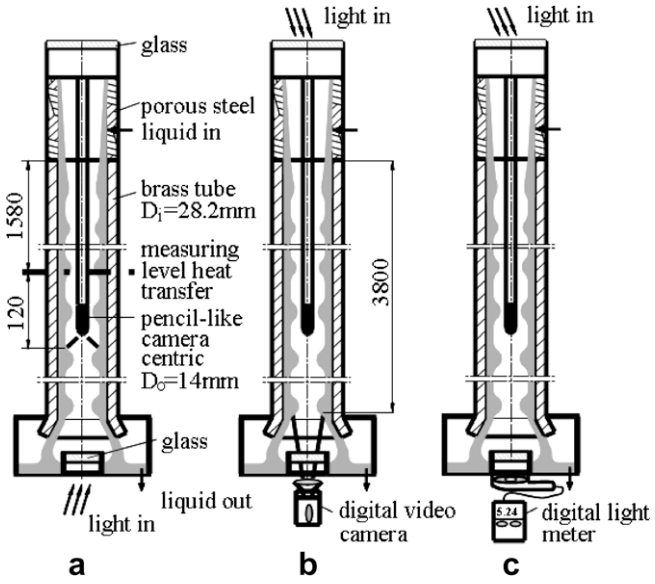

Fig. 4. Schematic drawing of the test rigs arrangements.

- A second arrangement, see Fig. 4b, was used to re-enact these measurements for comparison of wave types and frequencies at different positions along the tube. For this purpose a digital video camera (DVC, 50 s^{-1}) was positioned at the lower end of the tube with illumination from the upper end. Earlier investigations by Takamasa and Kobayashi (2000) with water (25 °C, Re = 80, inner tube diameter 26 mm) brought constant wave frequency for entrance lengths from 0.4 to 1.5 m where the large waves changed to small ones. In the present investigation, special lens systems allowed to move the focus along the lower part of the tube. This arrangement has been used for taking movies and photos with and without shear stress effects. Thereby two or rather three different liquid temperatures were adjusted, 14.6 and 37.9 °C with shear stress and additionally 47.3 °C without shear stress. The shear stress was realized by the vapour, created by heating the film separation device at the lower end of the tube, flowing upwards countercurrent to the liquid film.

While investigating the liquid film structure and varying the film temperature, photos have been taken at various film Re numbers offering a surprising result: The image brightness diminished for stepwise decreased film temperatures at a constant Re number, see Fig. 5. This has been found to be due to increasing wave heights, and there seems to be a correlation between wave shape and transmissivity of light, i.e. resulting image brightness.

- This phenomenon has further been investigated by application of a digital light meter (DLM, Luxmeter LX 1108, see Fig. 4c) replacing the DVC at the lower end as the third arrangement. By this, transmissivities (light intensity E) have been measured as the mean value during 4–10 min for various Re numbers (1.1–80) and temperatures (t = 15, 20, 25, and 30 °C). The temperature effect on the digital light meter and its sensor was investigated as well, and it could be excluded for the studied temperatures.

From the videos taken with the first two arrangements (Fig. 4a and b) wave shapes and effective wave frequencies have been evaluated as described in the next two sections.

3.2. Wave frequency evaluation

Visual observations were phased to discover specific wave characteristics of the falling liquid films depending on Re number and temperature. Fig. 5 shows photos taken by the DVC from the lower end of the tube in upward direction, see Fig. 4b, to give an idea of the images which subsequently have been evaluated with respect to wave structure and frequency. There are two series namely Re = 5 and 13, both of them taken with isopropanol at three different temperatures (47.3, 37.9, and 14.6 °C) representing different Ka numbers. The reader is asked to spend a short eye-training time and one will clearly discover differences in the wave height which becomes larger with increasing Re number and decreasing temperature.

Wave shape and effective wave frequency results have been evaluated for isopropanol and also for water with the latter ones taken with a second test rig, see Philipp et al. (2006). This has been done visually by counting wave crests, dark shadows of the waves, from slow motion PCC videos (50 half-frames per second) within an extended part of the inner tube perimeter (>1/6 of perimeter). Watching the slow motion videos frame by frame all moving shadows (waves) have been counted in the extended part, whether they have been a cycled or inclined line or only one larger cylindrical point.

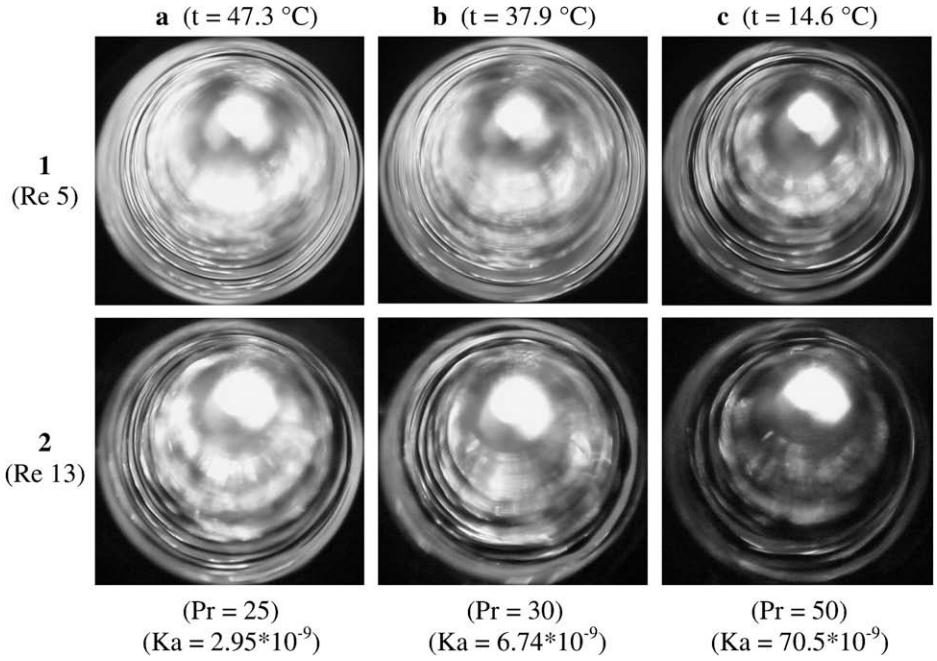

Fig. 5. Wavy film flow for isopropanol at different temperatures and Re numbers.

After these counting instructions and a short eye-training time, various persons (at least two) repeated counting several times at one and the same video sequence (3–6 s) for reducing scatter of the averaged frequency results. So an averaged accuracy of about ±4% was reached.

For reproducible results (evaluated from taken videos), firstly a best possible video quality is required, i.e. a definite and clearly visible image with maximum contrast realizable by different predefined aperture-settings. Additionally the illumination has to be optimized, i.e. no overexposure and huge reflections, wherefore the arrangement of illumination has been tested for the whole Re number section of investigation. An optimum (clearly visible image) was found with an indirect inclined illumination in the tube, and this was not changed during the measurements.

One example how to influence the clearly visible image (video): With increasing Re number the brightness of the image decreases because of growing wave heights wherefore the aperture has to be opened. The well-defined maximum of the opening width of the aperture is one limitation for the visual evaluation of frequency.

4. Results and discussion

4.1. Effective wave frequency without shear stress

Fig. 6 shows effective wave frequencies evaluated from the visual observations with the PCC, Fig. 4a, for isopropanol (t = 30.3 °C, two series) and water (t = 50 °C). The effective wave frequency is found to increase with the Re number. Characteristic curves have been obtained with local wave frequency maxima for both liquids. Respective peaks and representative shapes are indicated by thick solid curves. For both liquids the corresponding peaks have been numbered alphabetically (F–K) relating to the same wave shape. They are nearly on the same wave frequency level, with section "K" as an exception, and they will be discussed in the following with respect to the visual observations. One photo series, see Fig. 7, is added for illustration of related wave shape changes.

- *Peak F* (about Re = 8–9.5 in Fig. 6 in case of isopropanol, Re = 14–16.5 for water): At Re numbers below peak F two-dimensional waves are observed being not fully circled. These waves start to become irregular with occasional liquid mass accumulations when peak F is approached changing to a characteristic mass distribution beyond. These are first signs for fast waves and can be seen in Fig. 7 for Re = 9.4 and 9.9. The resulting image from the "top-view" has been sketched in Fig. 8 which is intended to illustrate the variations of the mass accumulation along the perimeter in Fig. 7.
- *Peak G* (Re = 10–11.8 and 17.5–21, respectively): With increasing Re numbers the irregular succession of waves and the related mass accumulations disappear, the two-dimensional characteristic without fully circled waves is still valid, however, with occasional inclinations of the wave crest. A wave deformation is observed close to peak G with an increase of height and a decrease of the lateral extension by about 1/4–1/3 of the tube perimeter, see Fig. 7 for Re = 11.7 and 12.4. The "fast running waves" are clearly visible at these Re numbers containing a large amount of liquid. The film surface is strongly influenced by overtaking of slower waves.
- *Peak H* (Re = 14–16 and 31–35, respectively): Wave shape is still two dimensional and almost all waves are inclined and not fully circled like a horseshoe, see Fig. 7 for Re = 14.4 and 15.9. With increasing Re number, waves more and more interleave each other and continuous transition from two to three-dimensional wave characteristic is observed. Waves exhibit regular mass accumulations in horizontal direction which can be described as a kind of basketwork, see Fig. 7 for Re = 17.3.
- *Peak I* (Re = 19–23 and 45–51, respectively): Transition from two- to three-dimensional wave shape is nearly completed. Periodic vertical wave displacement is observed with irregular succession of waves with respective transient accumulations when the waves interact and interleave each other. The basketwork profile is still present, see Fig. 7 Re = 17.3–20.3.
- *Peak J* (Re = 24–28 and 55–62, respectively): Wave shapes are fully three dimensional with increasing wave interferences and

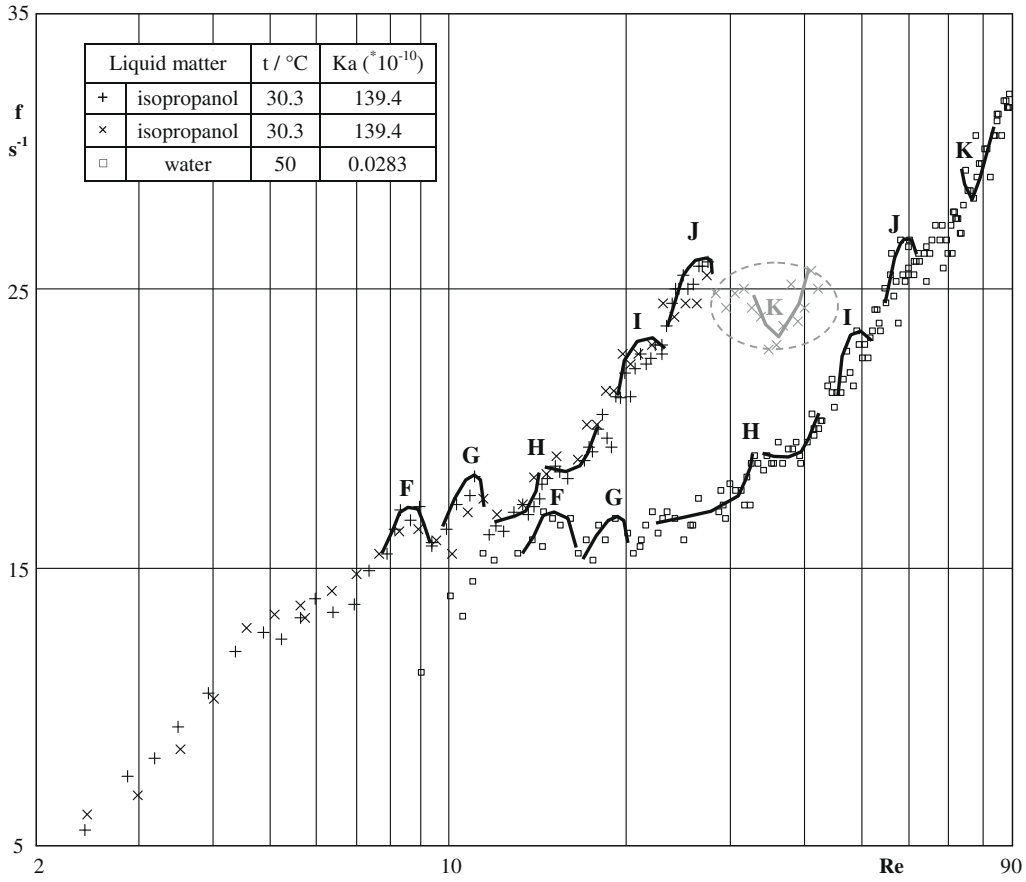

Fig. 6. Effective wave frequency versus Re number.

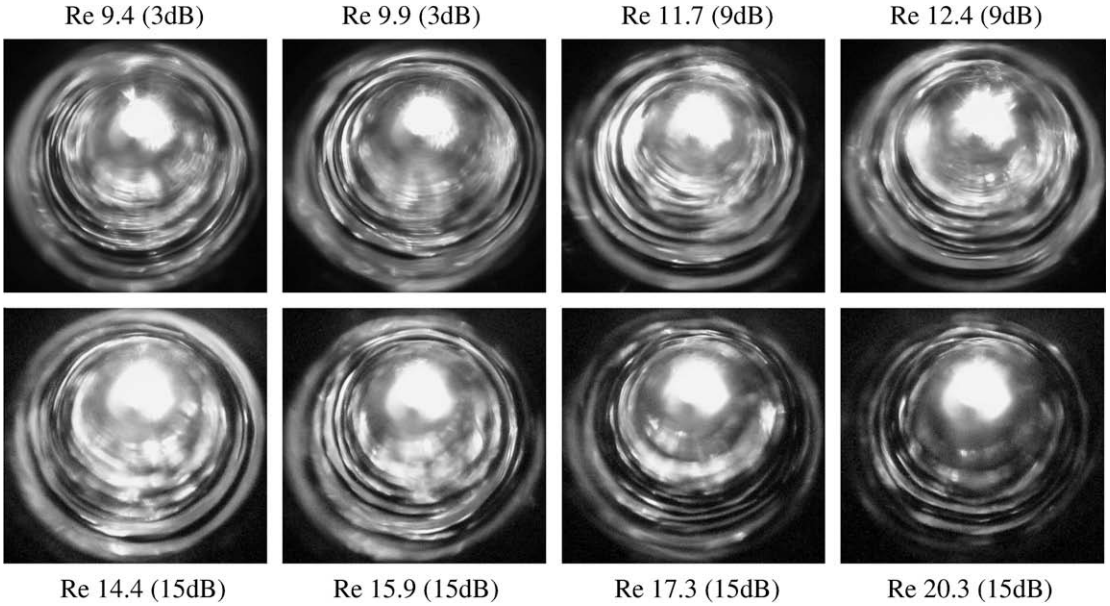

Fig. 7. Wavy film flow for isopropanol, t = 30.3 °C.

regular horizontal mass concentrations as observed earlier. Due to increasing wave interferences two distinct conditions of wave shapes and resulting wave frequencies are detectable. Furthermore, caused by large wave heights possibly some smaller waves are masked out, the wave frequency peak "J" (for isopropanol) is somewhat low in wave frequency. Thus the high wave frequency data points were used for indication by the thick solid curve.

Fig. 8. Schematic drawing of wave shape at Re = 9.9 and t = 30.3 °C.

– *Peak K* (Re = 32–40 and 74.5–81, respectively): The waves are in a persistent development and transition to turbulence with streak-like and surge-like waves starts. Adomeit (1996) and Adomeit and Renz (2000) observed these wave shapes, too.

The isopropanol data points encircled by a grey dotted ellipse are rather low in effective wave frequency caused by the large wave height and resulting bad illumination of the video section where smaller waves are masked out nevertheless showing a characteristic minimum.

Fig. 9a and b shows results of the transmissivity measurements, see Fig. 4c for the arrangement. Light intensity E (measured in l×) is plotted versus the Re number. Individual curves are obviously visible for each of the four selected temperatures 15, 20, 25, and 30 °C. Increasing the Re number starting with Re = 1 (at about E = 250 l×) brings monotonically decreasing transmissivities with variations of the slope. Evaluation of the obtained curves allows accurate conclusions for wave shape transitions at points A–L, see Table 2 where comprehensive explanations of changes in wave shapes are compiled. The transition points are in good agreement with the effective wave frequency maxima and minima in Fig. 6. Furthermore, the temperature effect upon wave shapes can be detected, and for rising temperatures displacement of the transition points to larger Re numbers and transmissivities are found and marked by ellipses (A–L). Contrary to expectations the transition point "J" is not definitely detectable that is why it is marked by a grey dotted ellipse.

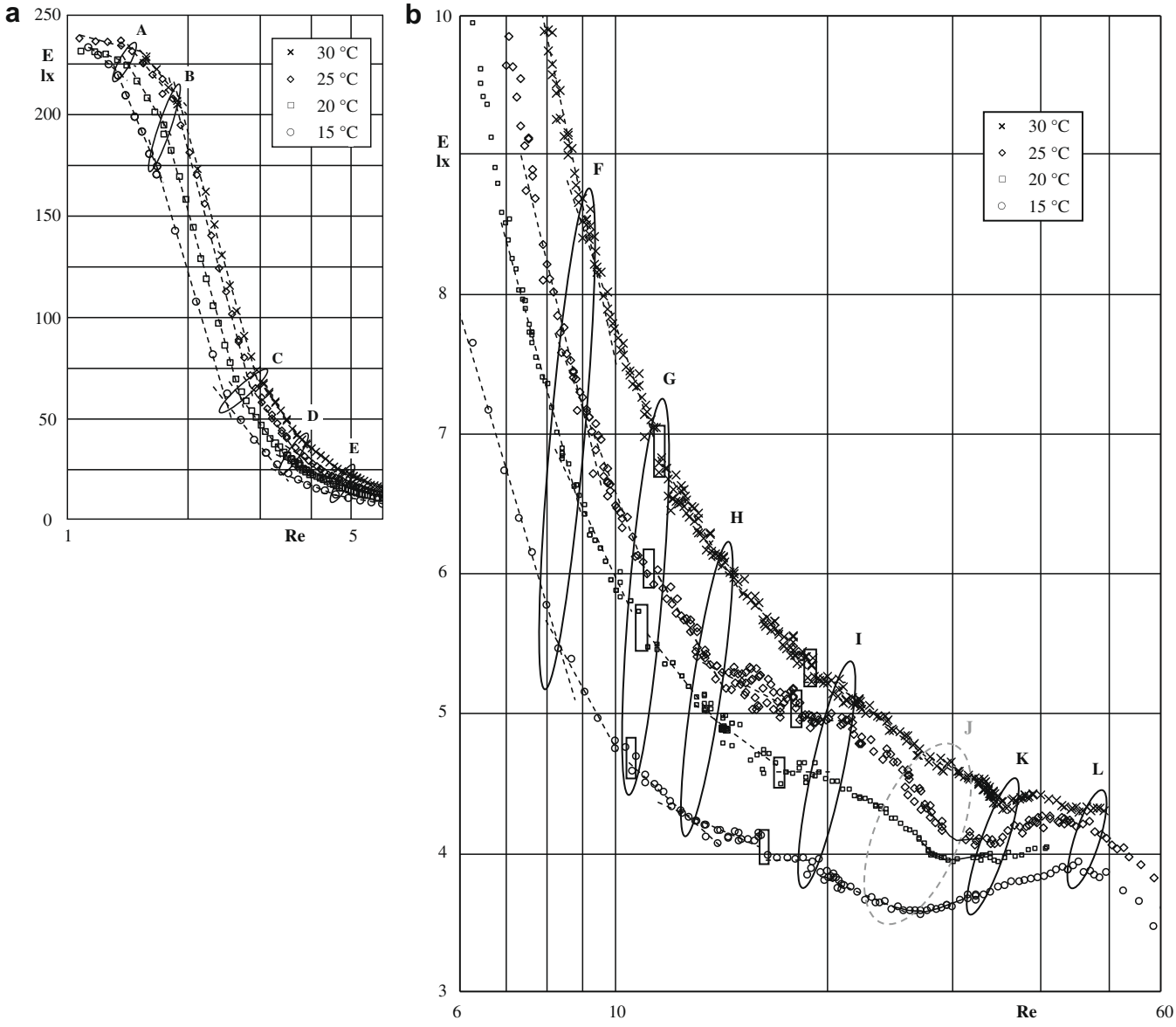

Fig. 9. (a and b) Light transmission versus Film Re number: (a) Re = 1–6 and (b) Re = 6–60.

Table 2
Detected and particularized changes in wave-shape and formation using a DLM.

No.	Isopropanol (Re)				Wave shape – formation and structure of falling film
	14.6 °C	20 °C	25 °C	30 °C	
A	1.31	1.39	1.43		A transition from laminar smooth film to laminar wavy film with very small waves can be observed.
B	1.64	1.74	1.84	1.86	The transition from laminar wavy film to first small waves is visible.
C	2.53	2.72	2.89	3.03	Furtheron small waves but with rising mightiness.
D	3.48	3.62	3.77	3.91	First large waves characterized by bow waves are visible.
E	4.5	4.72	4.85	5.0	A two-dimensional, not fully circled wave shape with an increase in number of bow waves and mightiness is visible.
F	8.3	8.6	8.8	9.1	Irregular wave-succession with wave-accumulations are first signals for "fast waves". Some circumferential mass concentration inside the waves gets started (Re 9.9 – see Figs. 7 and 8 (30 °C)).
G	10.5	10.9	11.2	11.6	Reduction of horizontal wave extent by about 1/4–1/3 is obviously visible. The wave shape is almost two-dimensional-inclined (relative to an inclined coordinate system) looking like a horseshoe. The irregular wave-succession stopped and an increase in wave-height is detectable.
H	12.6	13.4	14	14.7	The wave shape is almost 2-dimensional-inclined and the waves interleave themselves whereby a steadily transition from two- to three-dimensional wave shape is visible. The horizontal circumferential mass concentration inside the waves are nearly in regular distances over the extent.
I	18.5	19.5	20.6	21.4	The transition from two- to three-dimensional wave shape is nearly completed, the waves interleave and interact themselves. The wave shape can be described as a basketwork profile with periodic horizontal mass concentrations.
J	22.5–27.1	24.6–29.2	26.0–30.0	32.3	Fully three-dimensional wave shape with wave interferences and superposition.
K	31.6	33.1	35.1	36.5	The wave shape is fully three dimensional and first indications for a transition to turbulence are detectable.
L	45.4		47.6		The transition to turbulent wave shapes starts (streak-like and surge-like waves).

4.2. Correlation of heat transfer data

Wave factor results have been evaluated following Eq. (3) from the author's condensation heat transfer data at zero shear stress for water, ethanol and isopropanol, see Thumm et al. (2001), Gross et al. (2002) and Gross and Philipp (2006), and they are plotted in Fig. 10 versus the film Re number. A clear effect is seen for increasing Re and Ka numbers which yield remarkable intensifications of heat transfer in terms of the wave factor. After comparing these data with corresponding wave shape observations and evaluation of effective wave frequencies four characteristic ranges are encountered:

- Smallest wave factors amount to $F_{wave} = 1.028$, and they are obtained for water at Re < 7, i.e. in a range which is usually considered to be free of waves. Visual observations, however, showed occasional "very small" waves throughout with some limited effect on heat transfer.
- The next range is characterized by a strong increase of the wave factor up to about $F_{wave} = 1.345$. Two-dimensional waves are visually observed including small and large ones. Development of these waves is enhanced by increasing Re and Ka numbers. The first one (Re) is governed by film thickness and/or film velocity, while the second one (Ka) includes an increasing ratio of viscose to surface tension effects. The development of waves is promoted by the combined effects.
- Wave factors $1.345 \leqslant F_{wave} \leqslant 1.375$ are created by three-dimensional wave shapes, but the increase shows to be shallower.
- Wave factors $F_{wave} > 1.375$ characterize transition to local turbulence where the principle of combining laminar film theory with wave factors for consideration of heat transfer enhancement starts to loose its sense.

For the first three ranges the correlation of the condensation heat transfer data results in the following equations. They express the trend of wave factor with increasing Re number in the given limits:

$$\text{Range 1} \quad F_{wave} = 1.028 \quad (\mathrm{ReKa}^{0.09} < 0.8) \tag{4}$$

$$\text{Range 2} \quad F_{wave} = 1.096\mathrm{Re}^{0.141}\mathrm{Ka}^{0.0126} \quad (0.8 \leq \mathrm{ReKa}^{0.09} < 4.2) \tag{5}$$

$$\text{Range 3} \quad F_{wave} = 1.270\mathrm{Re}^{0.040}\mathrm{Ka}^{0.0036} \quad (4.2 \leq \mathrm{ReKa}^{0.09} < 7.3) \tag{6}$$

By fitting the measured data points in Eqs. (5) and (6), inclined lines were generated and together with a horizontal line due to the constant value of Eq. (4) added in Fig. 10.

4.3. Shear-stress effects

In practical applications like heat exchangers and chemical process columns, zero shear stress is just the limiting case for the condensing vapour being in cocurrent or countercurrent motion to the liquid film. The resulting shear stress influences film flow characteristics and heat transfer as well. Gross et al. (2002) and Gross and Philipp (2006) presented film condensation heat transfer experiments in the counter flow situation. Some of the isopropanol results are shown in Fig. 11 as Nu number versus the dimensionless shear stress τ^* at vapour–liquid interface.

In case of a smooth liquid film, e.g. Re = 0.68, the Nu number decreases with rising shear stress which is in excellent agreement with an analytical solution presented by Gross and Philipp (2006). This model is based on the balance of gravity, viscose and vapour-side shear forces to the liquid film

$$\mathrm{Re}_{film} = \frac{\delta_{film}^{+3}}{3} - \frac{\delta_{film}^{+2}}{2}\tau^* \tag{7}$$

where

$$\delta_{film}^{+} = \frac{\delta_{film}}{\left(\nu_{liq}^2/g\right)^{1/3}} \tag{8}$$

and

$$\tau^* = \frac{\tau}{g\left(\rho_{liq} - \rho_{vap}\nu_{liq}^2/g\right)^{1/3}} \tag{9}$$

are the dimensionless film thickness and dimensionless shear stress, respectively.

Application of Nusselt's theory

$$\mathrm{Nu} = \frac{h\left(\nu_{liq}^2/g\right)^{(1/3)}}{\lambda_{liq}} = \frac{1}{\delta_{liq}^{+}} \tag{10}$$

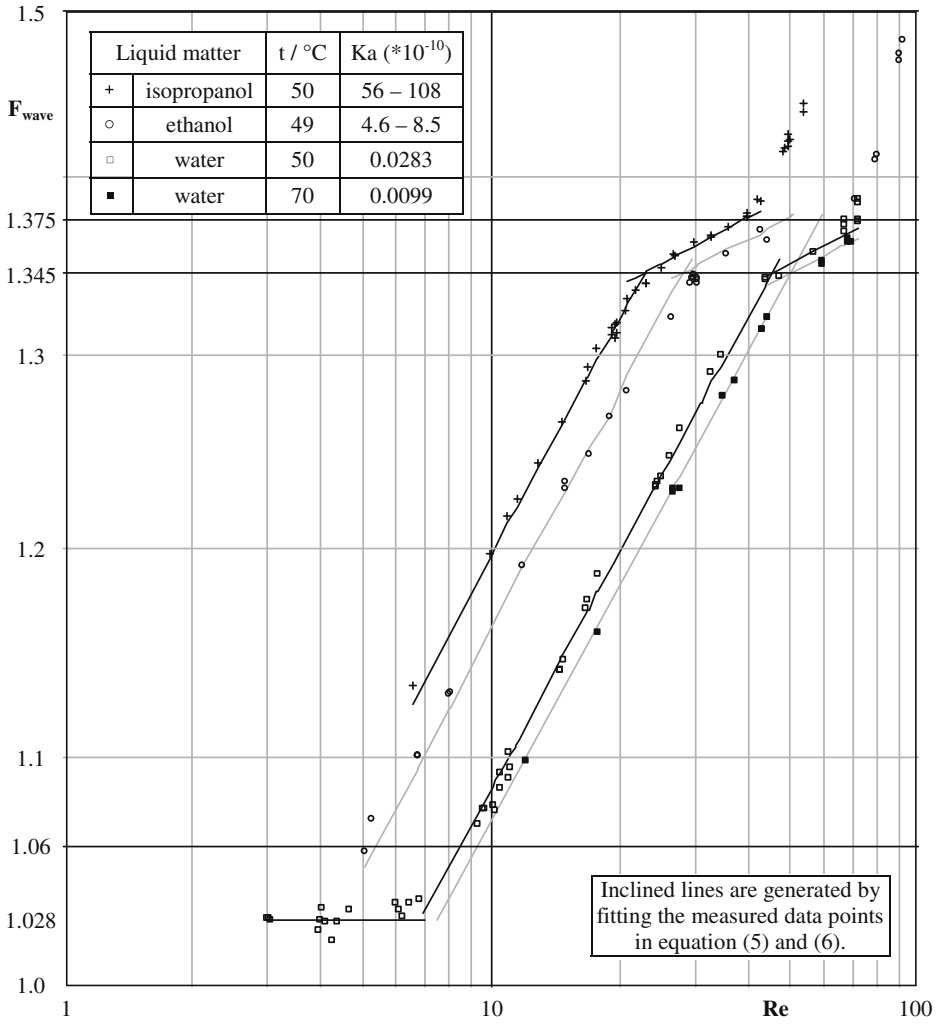

Fig. 10. Wave factor (condensation heat transfer data) versus Re number.

and an approximation, suggested by Thumm (2000) for cases with $0 < \tau^* < 3$, yields

$$\mathrm{Nu} = \left[0.59\tau^* + \left(3^{1/3} - 0.0086\tau^*\right)\left(\mathrm{Re}_{\mathrm{film}} + 0.28\tau^{*3}\right)^{1/3}\right]^{-1} \qquad (11)$$

which is plotted in Fig. 11 as an almost straight line.

This effect starts to be modified when the film Re number is increased, e.g. for Re = 1.4, still showing a decrease of Nu number for low shear stress cases. However, a minimum is obtained at about $\tau^* = 0.25$ with the transition to a re-increase of the Nu numbers. For even larger Re numbers the transition point is displaced to $\tau^* = 0.15$ (Re = 2.4) and finally to $\tau^* < 0.05$ for Re $\geqslant$ 6.7 at 25 °C. The transition shear stress and also the slope of the curves obviously depend on the temperature, i.e. on liquid film properties like the Ka number, as can be seen for Re = 6.5 at 50 °C where a weak minimum is found somewhere around $\tau^* = 0.3$ with a slight subsequent increase. This behaviour is strongly different from the case Re = 6.7 at 25 °C with the steep increase of Nu. An overview of the state-of-the-art in reflux condensation is given by Gross (2006).

In the present contribution countercurrent vapour-flow effects on the wave characteristics have been visually observed by the DVC, see Fig. 4b. With this camera position from below the wave-types could not be clearly defined as "small" or "large" ones. So we counted all visible waves, obviously resulting in a lower wave frequency than shown in Fig. 6. This is due to the fact that some small waves are masked out by larger ones.

In Fig. 12 frequencies of the visbile waves (f_{vw}), mainly large waves, are plotted versus the dimensionless shear stress for isopropanol at Re $\leqslant$ 30 (taken at 38 °C) covering the entire laminar-wavy flow regime. For Re < 9 the frequency is found to be not influenced by the shear stress in the limited range of investigation, however, at Re > 9 the wave frequency is clearly enhanced. The experiments have been repeated at a lower temperature (15 °C) where the lower limit for shear stress effects seems to be dislocated to smaller Re numbers. The detected wave frequency increase due to shear stress effects is coupled with a displacement of the wave shape regime. This has been visually observed and the frequency versus Re number plot, Fig. 13, shows respective results for both of the film temperatures under investigation. There are three classes of shear stress levels represented by hollow ($\tau^* = 0$), grey ($0.01 < \tau^* < 0.05$) and dark symbols ($0.05 < \tau^* < 0.08$). Keeping the Re number constant at Re $\geqslant$ 9 (for t = 38 °C), the frequency increase with τ^* can easily be seen. This is occasionally also found for t = 15 °C (Re = 5 and 13). Similarities of the wave shapes were observed at certain wave frequencies, whereby the data points with similar wave structures are encircled by ellipses (level (1): at about f_{vw} = 10–11 s^{-1}; level (2): at 12–13 s^{-1}; and level (3): at 15–16 s^{-1}) in Fig. 13. Level (1) is characterized by two-dimensional waves with bow waves being occasionally inclined and it corresponds to peak G in Fig. 6. For t = 15 °C this wave shape is obviously obtained at Re = 9 (for $\tau^* = 0$), but with shear stress it is already visible at Re = 5. Level

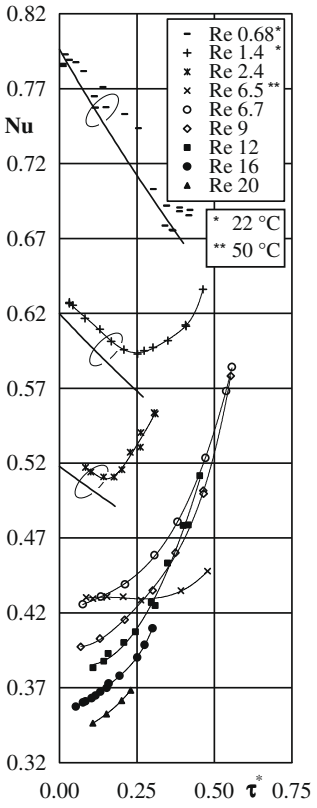

Fig. 11. Shear stress effect on heat transfer for isopropanol in the low Re number range.

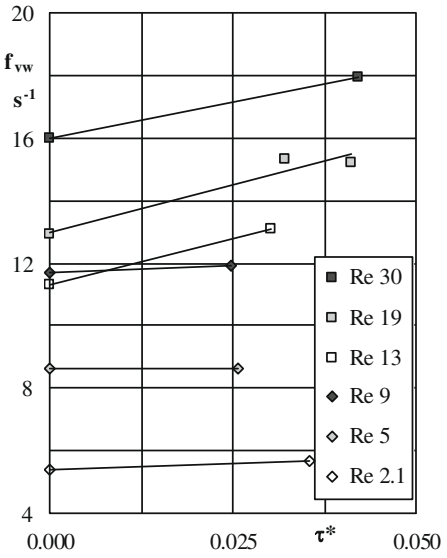

Fig. 12. Shear stress effect on large wave frequency for isopropanol at $t = 38$ °C.

(3) corresponds to peak H with the transition to three-dimensional wave structure as obtained at Re = 30 (for $\tau^* = 0$) and already at Re = 19 ($t = 38$ °C) with countercurrent vapour flow. This effect will now be considered from a different point of view, namely for constant Re = 5 ($t = 15$ °C): At $\tau^* = 0$ as the starting point, two dimensional, horizontal and not fully circled waves are observed (frequency $f_{vw} = 8.5\ s^{-1}$). An increase of shear stress supports transition to $f_{vw} = 10.5\ s^{-1}$ with inclined waves in some cases and occasional mass accumulations in horizontal direction. As a second example, Re = 19 ($t = 38$ °C) may be considered where shear stress promotes the transition from two- to three-dimensional waves and a respective frequency increase from 13 to $15\ s^{-1}$. Finally at Re = 30 ($t = 38$ °C) shear stress acts to a gradually transition to turbulence ($f_{vw} = 18\ s^{-1}$) starting from the three-dimensional film structure ($f_{vw} = 16\ s^{-1}$).

Despite the only small shear stress variations in the visual experiment which have been limited by the evaporation capabilities, Figs. 12 and 13 clearly show the observed increase of wave frequency and also the shift to a more structured liquid film for Re > 5 and $t = 38$ °C. The increase of wave frequency as seen in Fig. 12 for $\tau^* < 0.05$ is thought to be continued for larger shear stress resulting in a shear stress driven respective heat transfer enhancement as seen in Fig. 11. For the smallest Re number (Re = 0.68) no waves are expected with and without shear stress. The respective curve is well represented by the simple analytical model balancing gravity, viscose and shear forces, see Gross and Philipp (2006). For Re = 1.4 and 2.4 in Fig. 11, small shear stresses bring again no heat transfer effect in addition to that basic one, a fact which can easily be explained by diminishing effects on structure and frequency of the waves which are expected to be "small" ones and two-dimensional with the frequency in the order of $f_{vw} = 5\ s^{-1}$ (see Fig. 12). Shear stress effects on heat transfer enhancement are measurable for $\tau^* > 0.25$ (Re = 1.4) and $\tau^* > 0.15$ (Re = 2.4) respectively. The resulting heat transfer effect seems to be increased from Re 6.7 to 9 and further to Re = 12 brings an increasing slope of the curves in the Nu versus τ^* plot.

5. Conclusions

Earlier condensation heat transfer experiments of the present authors, Gross and Philipp (2006), have been evaluated and supplemented by visual investigations of falling liquid films.

For the limiting case of a stagnant vapour the enhancement of local heat transfer coefficients has been evaluated in terms of the wave factor. Correlations are obtained for three of four characteristic ranges of the wave activity: (1) so-called "small waves" at $\mathrm{ReKa}^{0.09} < 0.8$ bring heat transfer coefficients which exceed Nusselt's solution by about 2–3%; (2) for $0.8 \leq \mathrm{ReKa}^{0.09} < 4.2$, two-dimensional waves are found with wave factors ranging from 1.06 to 1.345; (3) transition to three-dimensional waves are obtained at $4.2 \leq \mathrm{ReKa}^{0.09} < 7.3$ with some additional but limited increase of the wave factor up to about 1.375; and (4) for even larger Re and/or Ka numbers transition to turbulence is observed making the principle of enhancement factors questionable.

Visual observations included the determination of wave frequencies from slow motion videos and light transmissivity measurements. Detailed characteristics of the wave frequency have been detected and up to 12 different changes of the wave structure are obtained. These transition points are found to be shifted to larger Re numbers when Ka is decreased. The wave structures are obtained as typical and reproducible maxima and minima when the wave frequency is plotted versus Re number.

For countercurrent vapour-flow a characteristic decrease and subsequent re-increase of heat transfer coefficients have been obtained for increasing shear stress. This has been found to be due to the wave activity which is negligible at smallest Re numbers where Nu number is found to follow a simple balance of gravity, viscose and shear forces. The wave activity, in terms of the wave frequency, is found to be enhanced for increasing shear stress, and the latter one promotes transition of, e.g. the wave structure from two to three-dimensional characteristic.

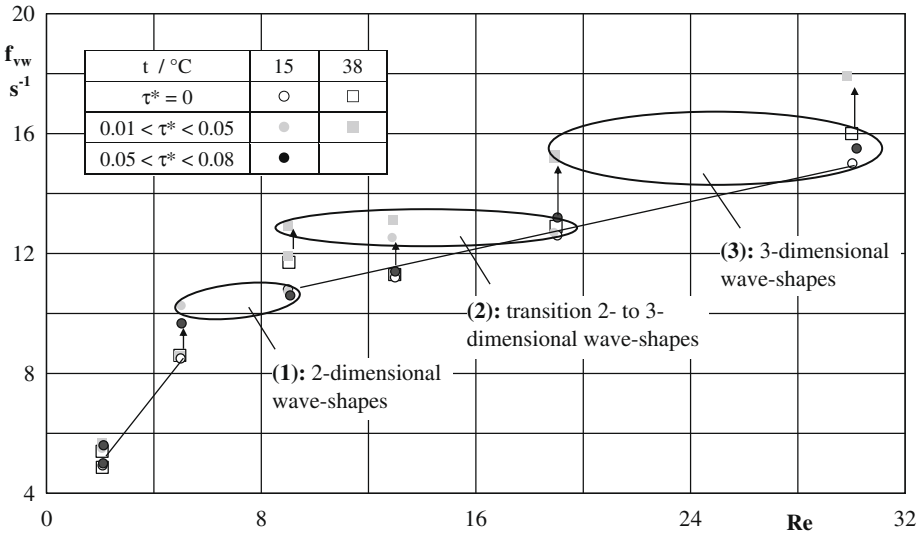

Fig. 13. Large wave frequency versus Re number with shear stress effects for isopropanol.

Acknowledgments

The authors like to thank Tobias Nell, Fernando Toshio Okamura (São Paulo, Brazil) and Anjali Bhide (IIT Madras, India) for their assistance. The support by the Deutsche Forschungsgemeinschaft (DFG) is greatly appreciated.

References

Adomeit, P., 1996. Experimentelle Untersuchung der Strömung laminar-welliger Rieselfilme, Ph.D. Thesis, RWTH Aachen, Germany.
Adomeit, P., Renz, U., 2000. Hydrodynamics of three-dimensional waves in laminar falling films. Int. J. Multiphase Flow 26, 1183–1208.
Adomeit, P., Leefken, A., Renz, U., 2000. Experimental and numerical investigations on wavy films. In: Proceeding of the Third European Thermal Science Conference, vol. 2, pp. 1003–1009.
Alekseenko, S.V., Nakoryakov, V.E., Pokusaev, B.G., 1994. Wave flow of liquid films. Begell House, New York, Wallingford.
Alhusseini, A.A., Tuzla, K., Chen, J.C., 1997. Falling film evaporation of single component liquids. Int. J. Heat Mass Transfer 41, 1623–1632.
Al-Sibai, F., 2004. Experimentelle Untersuchung der Strömungscharakteristik und des Wärmeübergangs bei welligen Rieselfilmen, Ph.D. Thesis, RWTH Aachen, Germany.
Al-Sibai, F., Leefken, A., Renz, U., 2002a. Local and instantaneous distribution of heat transfer rates and velocities in thin wavy films. In: Proceedings of the Eurotherm 71 on Visualization, Imaging Data Analysis in Convective Heat and Mass Transfer LTM-UTAP, Universite de Reims France 71, pp. 83–94.
Al-Sibai, F., Leefken, A., Renz, U., 2002b. Local and instantaneous distribution of heat transfer rates through wavy films. Int. J. Therm. Sci. 41, 658–663.
Ambrosini, W., Forgione, N., Oriolo, F., 2002. Statistical characteristics of water film falling down a flat plate at different inclinations and temperatures. Int. J. Multiphase Flow 28, 1521–1540.
Blangetti, F., 1984. VDI-Wärmeatlas, Section Ja. VDI-Verlag, Düsseldorf.
Brauer, H., 1956. Strömung und Wärmeübergang bei Rieselfilmen, VDI-Forsch.-Heft 457, Düsseldorf.
Brauer, H., 1971. Grundlagen der Einphasen- und Mehrphasenströmungen, Verlag Sauerländer, Aarau und Frankfurt am Main.
Chun, K.J., Seban, R.A., 1971. Heat transfer to evaporating liquid films. J. Heat Transfer 93, 391–396.
Clark, W.W., 2002. Liquid film thickness measurement. Multiphase Sci. Technol. 14, 1–74.
Drosos, E.I.P., Paras, S.V., Karabelas, A.J., 2004. Characteristics of developing free falling films at intermediate Reynolds and high Kapitza numbers. Int. J. Multiphase Flow 30, 853–876.
Dukler, A.E., Bergelin, O.P., 1952. Characteristics of flow in falling films. Chem. Eng. Prog. 48, 557–563.
Emmons, H.W., 1951. The laminar–turbulent transition in a boundary layer. J. Aeronaut. Sci. 18, 490–498.
Grimley, S.S., 1945. Liquid film flow conditions in packed towers. Trans. Inst. Chem. Eng. 23, 228–235.
Gross, U., 2006. Shear stress effects on countercurrent film condensation inside tubes: a review of recent developments 90 years after Nusselt. In: Proceedings of the 13th International Heat Transfer Conference, Sydney, CD, ISBN 1-56700-226-9.
Gross, U., Philipp, Ch., 2006. Conjugated shear stress and Prandtl number effects on reflux condensation heat transfer inside a vertical tube. Int. J. Heat Mass Transfer 49, 144–153.
Gross,U., Philipp, Ch., Thumm, S., 2002. Effect of countercurrent vapour flow on film condensation heat transfer inside a vertical tube. In: Proceedings of the 12th International Heat Transfer Conference, Grenoble, pp. 923–928.
Ishigai, S., Nakanisi, S., Koizumi, T., Oyabu, Z., 1972. Hydrodynamics and heat transfer of vertical falling liquid films. Bull. JSME 15, 594–602.
Kapitza, P.L., 1948. Wave flow of a thin viscous layer. I. Free flow. J. Exp. Theor. Phys. 18, 3–20.
Karapantsios, T.D., Karabelas, A.J., 1995. Longitudinal characteristics of wavy falling films. Int. J. Multiphase Flow 1, 119–127.
Karapantsios, T.D., Paras, S.V., Karabelas, A.J., 1989. Statistical characteristics of free falling films at high Reynolds number. Int. J. Multiphase Flow 1, 1–21.
Koizumi, Y., Ohtake, H., Ikeda, S., 2000. Characteristics of a falling liquid film on the outer surface of a vertical pipe (minimum wetting rates and waves on the film) ASME International Mechanical Engineering Congress and Exposition. Proc. Heat Transfer Div. 2, 197–203.
Koizumi, Y., Ohtake, H., Ikeda, S., 2001. Characteristics of an R-113 falling liquid film on the outer surface of a vertical pipe. In: Proceedings of the Fourth International Conference on Multiphase Flow, CD-ROM.
Koizumi, Y., Enari, R., Ohtake, M., 2005. Correlations of characteristics of waves on a film falling down on a vertical wall. In: Proceedings of the ASME, IMECE.
Kutateladze, S.S., 1963. Fundamentals of Heat Transfer. Verlag E. Arnold, London. 307.
Labuntsov, D.A., 1957. Heat transfer in film condensation of pure vapours on vertical surfaces and horizontal tubes. Teploenergetika 7, 72–80.
Lel, V.V., Al-Sibai, F., Leefken, A., Renz, U., 2005. Local thickness and wave velocity measurement of wavy films with a chromatic confocal imaging method and a fluorescence intensity technique. Exp. Fluid 39, 856–864.
Leuthner, S., 1999. Messung und Modellierungen zum Energie- und Stofftransport in Fallfilmen. Fortschr.-Ber. VDI Reihe 3 Nr. 594, VDI Verlag Düsseldorf.
McAdams, W.H., 1954. Heat Transmission. McGraw-Hill, New York.
Mitrovic, J., 1990. Filmkondensation ruhender Dämpfe an senkrechten Flächen. BWK 42, 598–609.
Nusselt, W., 1916. Die Oberflächenkondensation des Wasserdampfs. Z. Ver. Dt. Ing. 60, 541–546. and 569-575.
Park, C.D., Nosoko, T., 2003. Three-dimensional wave dynamics on a liquid falling film and associated mass transfer. AIChE J. 49, 2715–2727.
Park, C.D., Nosoko, T., Gima, S., Ro, S.T., 2004. Wave-augmented mass transfer in a liquid film falling inside a vertical tube. Int. J. Heat Mass Transfer 47, 2587–2598.
Philipp, Ch., Doeg, A., Kufaas Tellefsen, S., Gross, U., 2006. Wave characteristics of liquid films – correlation of heat transfer data with visual observations. In: Proceedings of the 13th International Heat Transfer Conference, Sydney, CD, ISBN 1-56700-226-9.
Portalski, S., 1960. The mechanism of flow in wetted wall columns, Ph.D. Thesis, London University.
Portalski, S., 1963. Studies of falling liquid films. Chem. Eng. Sci. 18, 787–804.
Portalski, S., 1973. Phase velocities on liquid films flowing on a smooth vertical plate. AIChE J. 19, 1244–1246.

Schagen, A., Modigell, M., Dietze, G., Kneer, R., 2006. Simultaneous measurement of local film thickness and temperature distribution in wavy liquid films using a luminescence technique. Int. J. Heat Mass Transfer 49, 5049–5061.

Sofrata, H., 1980. Theoretical study of filmwise condensation considering wave initiation. Wärme- und Stoffübertragung 14, 201–210.

Takahama, H., Kato, S., 1980. Longitudinal flow characteristics of vertically falling liquid films without concurrent gas flow. Int. J. Multiphase Flow 6, 203–215.

Takamasa, T., Hazuku, T., 2000. Measuring interfacial waves on film flowing down a vertical plate in the entry region using laser focus displacement meters. Int. J. Heat Mass Transfer 43, 2807–2819.

Takamasa, T., Kobayashi, K., 2000. Measuring interfacial waves on film flowing down tube inner wall using laser focus displacement meter. Int. J. Mutiphase Flow 26, 1493–1507.

Thumm, S., 2000. Filmkondensation im senkrechten Rohr bei Gegenstrom von Dampf und Flüssigkeit, Ph.D. Thesis, TU Bergakademie Freiberg, Germany.

Thumm, S., Philipp, Ch., Gross, U., 2001. Film condensation of water in a vertical tube with countercurrent vapour flow. Int. J. Heat Mass Transfer 44, 4245–4256.

Uehara, H. et al., 1980. In: Proceedings of the 17th National Heat Transfer Symposium of Japan, 1980, p. 427.

Uehara, H., Kusuda, H., Nakaoka, T., Yamada, M., 1983. Experimental study of filmwise condensation on a vertical surface. Nipponkikaigakkai Ronbunshu. Trans. Jpn. Soc. Mech. Eng. B 49, 666–675.

Uehara, H., Nakaoka, T., Murata, K., Egashira, S., 1988. Body forced convection condensation on a vertical smooth surface: 1st report, flow pattern of condensate film and local heat transfer coefficient. Trans. Jpn. Soc. Mech. Eng. B 54, 2537–2544.

Uehara, H., Nakaoka, T., Egashira, S., Taguchi, Y., 1989. Body forced convection condensation on a vertical smooth Surface: 2nd report, flow patterns of condensate film and mean heat transfer coefficients. Trans. Jpn. Soc. Mech. Eng. B 55, 442–449.

VDI Wärmeatlas, 2006. In: Ing. H. Martin (Ed.), Dimensionslose Kenngrößen, 10th Edition, Section Bc 1-Bc 3, Springer Verlag, Heidelberg.

Wilke, W., 1962. Wärmeübergang an Rieselfilme. VDI-Forschungsheft 490. VDI-Verlag, Düsseldorf.

Yu, L.-Q., Wasden, F.K., Dukler, A.E., Balakotaiah, V., 1995. Nonlinear evolution of waves on falling films at high Reynolds numbers. Phys. Fluids 7, 1886–1902.

Zozulya, N.V., 1959. Investigation of heat transfer with vapor condensation in vertical tubes. In: Heat transfer and thermal modelling (in Russian). Izv. Akad. Nauk SSSR, Moscow, pp. 287–297.

Zhivaikin, L.Y., Volgin, B.P., 1961. The determination of the amount of liquid carried away from the surface of a film of a gas flow. J. Eng. Phys. Thermophys. 4, 114.